Lattice QCD with an inhomogeneous magnetic field background

Lattice conference 2022, Bonn, Germany

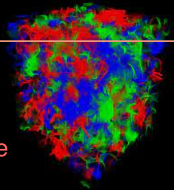

Dean Valois
dvalois@physik.uni-bielefeld.de

Gergely Endrődi   Bastian Brandt   Gergely Marko   Francesca Cuteri

August 12, 2022

Physics Department
Bielefeld University

Outline

1. Strongly magnetized physical systems
2. Magnetic field on the lattice
3. Lattice simulations
4. Summary & Conclusions

Strongly magnetized physical systems

STRONGLY MAGNETIZED PHYSICAL SYSTEMS

QCD vacuum

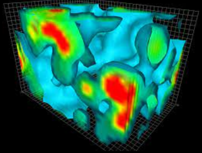

Strongly magnetized physical systems

QCD vacuum

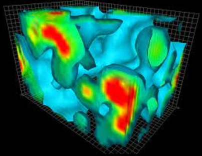

Early universe

$\sqrt{eB} \sim 1.5$ GeV

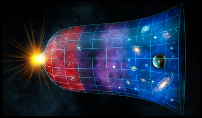

STRONGLY MAGNETIZED PHYSICAL SYSTEMS

QCD vacuum

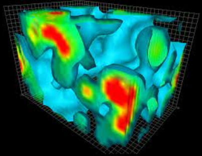

Early universe

$\sqrt{eB} \sim 1.5$ GeV

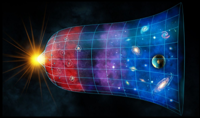

Neutron stars

$\sqrt{eB} \sim 1$ MeV

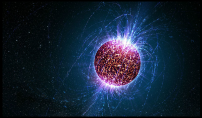

Strongly magnetized physical systems

QCD vacuum

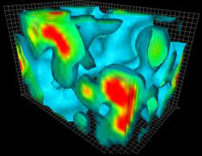

Early universe

$\sqrt{eB} \sim 1.5$ GeV

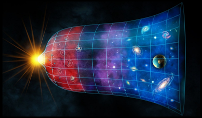

Neutron stars

$\sqrt{eB} \sim 1$ MeV

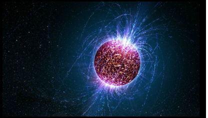

Heavy-ion collision

$\sqrt{eB} \sim 0.5$ GeV

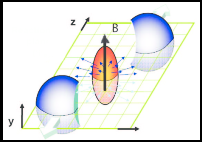

Strongly magnetized physical systems

QCD vacuum

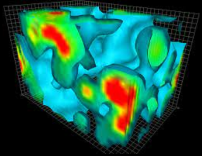

Early universe

$\sqrt{eB} \sim 1.5$ GeV

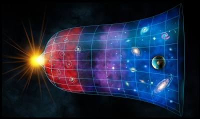

Neutron stars

$\sqrt{eB} \sim 1$ MeV

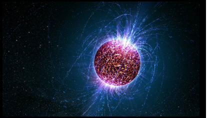

Heavy-ion collision

$\sqrt{eB} \sim 0.5$ GeV

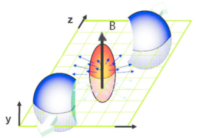

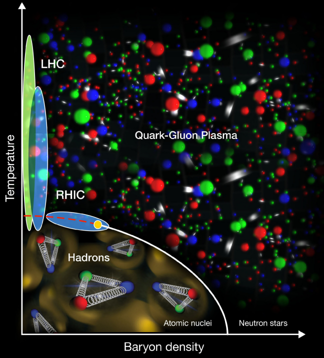

Magnetic fields in heavy-ion collisions

Magnetic fields in heavy-ion collisions

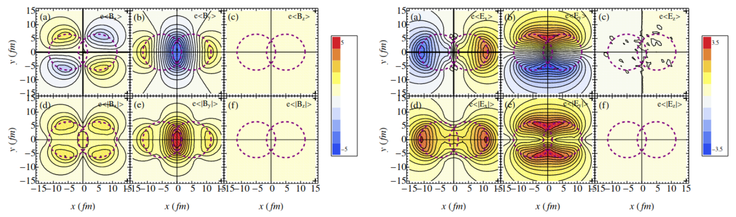

Figure 2: Spatial distributions of the electric (right) and magnetic (left) fields for an impact parameter $b = 10$ fm Deng and Huang 2012.

Magnetic fields in heavy-ion collisions

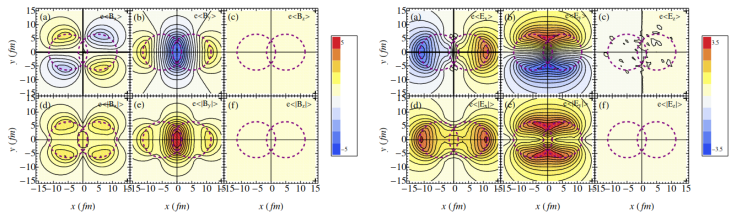

Figure 2: Spatial distributions of the electric (right) and magnetic (left) fields for an impact parameter $b = 10$ fm Deng and Huang 2012.

Caveats:

1. **B** and **E** are highly non-homogeneous.

Magnetic fields in heavy-ion collisions

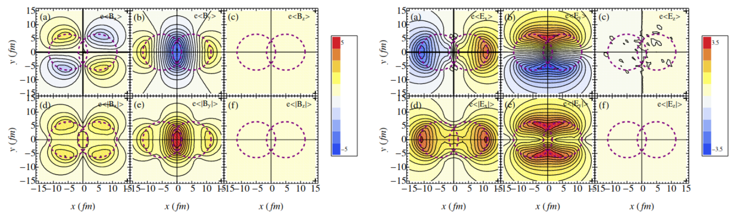

Figure 2: Spatial distributions of the electric (right) and magnetic (left) fields for an impact parameter $b = 10$ fm Deng and Huang 2012.

Caveats:

1. **B** and **E** are highly non-homogeneous.
2. A real **E** leads to sign problem.

Magnetic fields in heavy-ion collisions

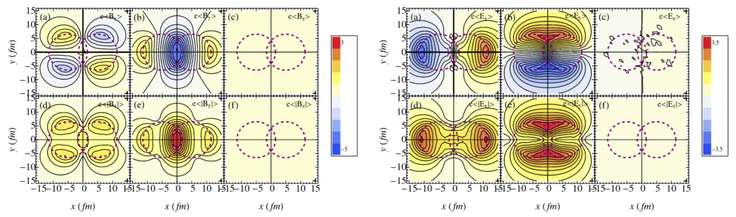

Figure 2: Spatial distributions of the electric (right) and magnetic (left) fields for an impact parameter $b = 10$ fm Deng and Huang 2012.

Caveats:

1. **B** and **E** are highly non-homogeneous.
2. A real **E** leads to sign problem.
3. No Minkoswki time evolution from Euclidean simulations.

Magnetic fields in heavy-ion collisions

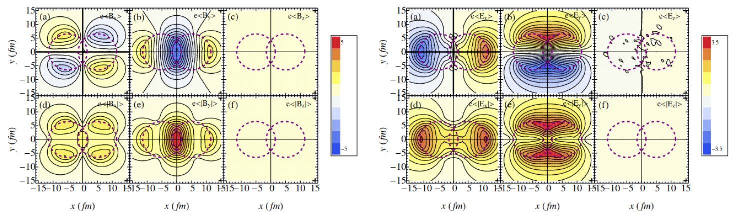

Figure 2: Spatial distributions of the electric (right) and magnetic (left) fields for an impact parameter $b = 10$ fm Deng and Huang 2012.

Caveats:

1. **B** and **E** are highly non-homogeneous.
2. A real **E** leads to sign problem.
3. No Minkoswki time evolution from Euclidean simulations.

What can we do?

MAGNETIC FIELDS IN HEAVY-ION COLLISIONS

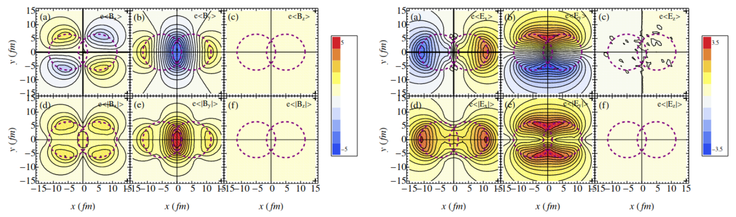

Figure 2: Spatial distributions of the electric (right) and magnetic (left) fields for an impact parameter $b = 10$ fm Deng and Huang 2012.

Caveats:

1. **B** and **E** are highly non-homogeneous.
2. A real **E** leads to sign problem.
3. No Minkowski time evolution from Euclidean simulations.

What can we do?

$B(x)$ as background in lattice QCD!

Magnetic field on the lattice

Uniform magnetic field on the lattice

$$\boxed{qB = \frac{2\pi N_b}{L_x L_y}, \quad N_b \in \mathbb{Z}}$$

Uniform magnetic field on the lattice

gluon field $\longrightarrow U_\mu \in$ SU(3)

$$\boxed{qB = \frac{2\pi N_b}{L_x L_y}, \quad N_b \in \mathbb{Z}}$$

Uniform magnetic field on the lattice

gluon field $\longrightarrow U_\mu \in$ SU(3)
magnetic field $\longrightarrow u_\mu = e^{iaqA_\mu} \in$ U(1)

$$\boxed{qB = \frac{2\pi N_b}{L_x L_y}, \quad N_b \in \mathbb{Z}}$$

Uniform magnetic field on the lattice

gluon field $\longrightarrow U_\mu \in$ SU(3)
magnetic field $\longrightarrow u_\mu = e^{iaqA_\mu} \in$ U(1)

$$\boxed{qB = \frac{2\pi N_b}{L_x L_y}, \quad N_b \in \mathbb{Z}}$$

Construction of the links:

$$\mathbf{B} = \nabla \times \mathbf{A}$$

$$A_y = Bx \qquad A_x = A_z = A_t = 0$$

UNIFORM MAGNETIC FIELD ON THE LATTICE

gluon field $\longrightarrow U_\mu \in$ SU(3)

magnetic field $\longrightarrow u_\mu = e^{iaqA_\mu} \in$ U(1)

$$\boxed{qB = \frac{2\pi N_b}{L_x L_y}, \quad N_b \in \mathbb{Z}}$$

Construction of the links:

$$\mathbf{B} = \nabla \times \mathbf{A}$$

$$A_y = Bx \qquad A_x = A_z = A_t = 0$$

$$u_x = \begin{cases} e^{-iqBL_x y} & \text{if } x = L_x - a \\ 1 & \text{if } x \neq L_x - a \end{cases}$$

$$u_y = \; e^{iaqBx} \quad 0 \leq x \leq L_x - a$$

$$u_z = u_t = 1$$

INHOMOGENEOUS MAGNETIC FIELD ON THE LATTICE

$$\mathbf{B} = \frac{B}{\cosh\left(\frac{x-L_x/2}{\epsilon}\right)^2}\hat{z}$$

Profile motivated by heavy-ion collision scenarios Deng and Huang 2012, Cao 2018.

$$\boxed{qB = \frac{\pi N_b}{L_y \epsilon \tanh\left(\frac{L_x}{2\epsilon}\right)} \qquad N_b \in \mathbb{Z}}$$

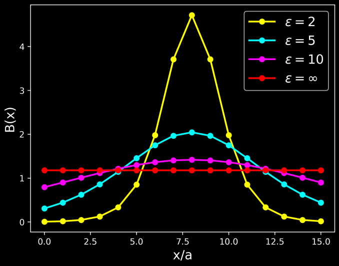

$$u_x = \begin{cases} e^{-2iqB\epsilon y \tanh\left(\frac{L_x}{2\epsilon}\right)} & \text{if } x = L_x - a \\ 1 & \text{if } x \neq L_x - a \end{cases}$$

$$u_y = e^{iaqB\epsilon\left[\tanh\left(\frac{x-L_x/2}{\epsilon}\right)+\tanh\left(\frac{L_x}{2\epsilon}\right)\right]}, \quad 0 \leq x \leq L_x - a$$

$$u_z = u_t = 1$$

Lattice simulations

The simulation set up

THE SIMULATION SET UP

- Improved staggered fermions with $N_f = 2 + 1$ flavors and physical masses;

The simulation set up

- Improved staggered fermions with $N_f = 2+1$ flavors and physical masses;
- Lattices: $16^3 \times 6 \quad 24^3 \times 8 \quad 28^3 \times 10 \quad 36^3 \times 12 \quad \longrightarrow$ continuum limit (lattice spacing $\to 0$, $V =$ const.);

The simulation set up

- Improved staggered fermions with $N_f = 2 + 1$ flavors and physical masses;
- Lattices: $16^3 \times 6 \quad 24^3 \times 8 \quad 28^3 \times 10 \quad 36^3 \times 12 \quad \longrightarrow$ continuum limit (lattice spacing $\to 0$, $V =$ const.);
- Number of gauge confiigurations $\sim \mathcal{O}(200)$ - $\mathcal{O}(700)$;

THE SIMULATION SET UP

- Improved staggered fermions with $N_f = 2 + 1$ flavors and physical masses;
- Lattices: $16^3 \times 6 \quad 24^3 \times 8 \quad 28^3 \times 10 \quad 36^3 \times 12 \quad \longrightarrow$ continuum limit (lattice spacing $\to 0$, $V =$ const.);
- Number of gauge confiigurations $\sim \mathcal{O}(200)$ - $\mathcal{O}(700)$;
- Magnetic field

$$\mathbf{B} = \frac{B}{\cosh\left(\frac{x - L_x/2}{\epsilon}\right)^2}\hat{z} \qquad eB = \frac{3\pi N_b}{L_y \epsilon \tanh\left(\frac{L_x}{2\epsilon}\right)} \qquad \epsilon \approx 0.6 \text{ fm}$$

strength 0 GeV $\leq \sqrt{eB} \leq 1.2$ GeV;

THE SIMULATION SET UP

- Improved staggered fermions with $N_f = 2+1$ flavors and physical masses;
- Lattices: $16^3 \times 6 \quad 24^3 \times 8 \quad 28^3 \times 10 \quad 36^3 \times 12 \quad \longrightarrow$ continuum limit (lattice spacing $\to 0$, $V =$ const.);
- Number of gauge confiigurations $\sim \mathcal{O}(200)$ - $\mathcal{O}(700)$;
- Magnetic field

$$\mathbf{B} = \frac{B}{\cosh\left(\frac{x - L_x/2}{\epsilon}\right)^2}\hat{z} \qquad eB = \frac{3\pi N_b}{L_y \epsilon \tanh\left(\frac{L_x}{2\epsilon}\right)} \qquad \epsilon \approx 0.6 \text{ fm}$$

strength 0 GeV $\leq \sqrt{eB} \leq 1.2$ GeV;

- Temperature range 68 MeV $\leq T \leq 300$ MeV (crossover transition at $T_c \sim 155$ MeV).

Lattice observables

LATTICE OBSERVABLES

- Local chiral condensates (**u** and **d** quarks!)

$\bar{\psi}\psi$

Lattice observables

- Local chiral condensates (**u** and **d** quarks!)

$$\bar{\psi}\psi \xrightarrow{\text{renormalization}} \Sigma(x,T,B) = \frac{m_{ud}}{m_\pi^4}\left[\bar{\psi}\psi(x,T,B) - \bar{\psi}\psi(x,T,0)\right]$$

Lattice observables

- Local chiral condensates (**u** and **d** quarks!)

$$\bar{\psi}\psi \xrightarrow{\text{renormalization}} \Sigma(x,T,B) = \frac{m_{ud}}{m_\pi^4}\left[\bar{\psi}\psi(x,T,B) - \bar{\psi}\psi(x,T,0)\right]$$

- Local Polyakov loop

$$P = \frac{1}{L_x L_y}\sum_{y,z} \mathrm{Re}\,\mathrm{Tr}\prod_n U_t(x,y,z,n)$$

Lattice observables

- Local chiral condensates (**u** and **d** quarks!)

$$\bar{\psi}\psi \quad \xrightarrow{\text{renormalization}} \quad \Sigma(x,T,B) = \frac{m_{ud}}{m_\pi^4}\left[\bar{\psi}\psi(x,T,B) - \bar{\psi}\psi(x,T,0)\right]$$

- Local Polyakov loop

$$P = \frac{1}{L_x L_y}\sum_{y,z} \mathrm{Re}\,\mathrm{Tr}\prod_n U_t(x,y,z,n) \quad \xrightarrow{\text{renormalization}} \quad \frac{P(x,T,B)}{P(x,T,0)}$$

Lattice observables

- Local chiral condensates (u and d quarks!)

$$\bar{\psi}\psi \xrightarrow{\text{renormalization}} \Sigma(x,T,B) = \frac{m_{ud}}{m_\pi^4}\left[\bar{\psi}\psi(x,T,B) - \bar{\psi}\psi(x,T,0)\right]$$

- Local Polyakov loop

$$P = \frac{1}{L_x L_y}\sum_{y,z} \mathrm{Re}\,\mathrm{Tr}\prod_n U_t(x,y,z,n) \xrightarrow{\text{renormalization}} \frac{P(x,T,B)}{P(x,T,0)}$$

- Local electric currents (u, d and s quarks!)

$$\langle\, J_i(x)\,\rangle = e\left\langle\, \frac{2}{3}\bar{u}\gamma^i u - \frac{1}{3}\bar{d}\gamma^i d - \frac{1}{3}\bar{s}\gamma^i s\,\right\rangle$$

CHIRAL CONDENSATE - $\Sigma(T,B) = \frac{m_{ud}}{m_\pi^4}[\bar{\psi}\psi(T,B) - \bar{\psi}\psi(T,0)]$

CHIRAL CONDENSATE - $\Sigma(T,B) = \frac{m_{ud}}{m_\pi^4}[\bar\psi\psi(T,B) - \bar\psi\psi(T,0)]$

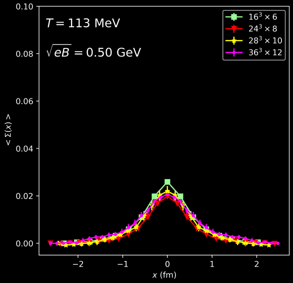

Chiral condensate - $\Sigma(T,B) = \frac{m_{ud}}{m_\pi^4}[\bar{\psi}\psi(T,B) - \bar{\psi}\psi(T,0)]$

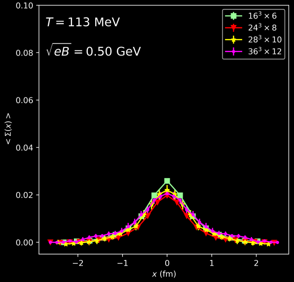

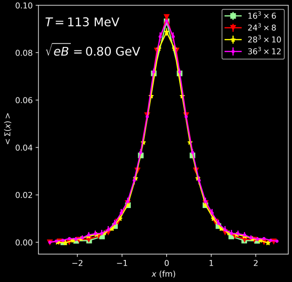

Chiral condensate - $\Sigma(T,B) = \frac{m_{ud}}{m_\pi^4}[\bar\psi\psi(T,B) - \bar\psi\psi(T,0)]$

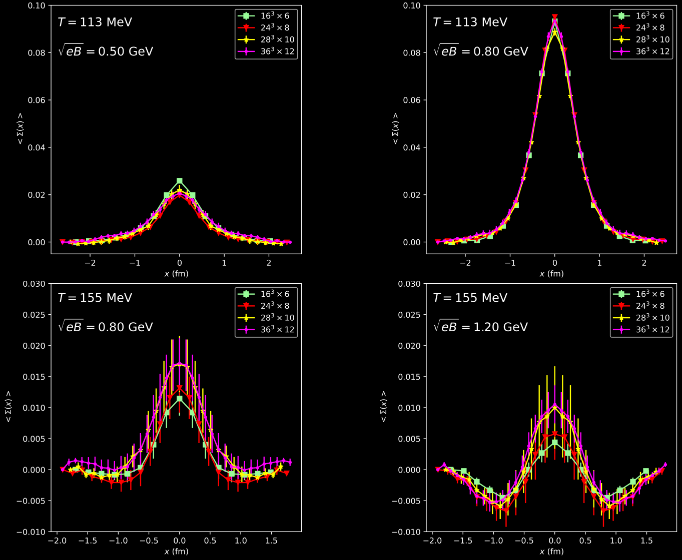

Chiral condensate - $\Sigma(T,B) = \frac{m_{ud}}{m_\pi^4}[\bar\psi\psi(T,B) - \bar\psi\psi(T,0)]$

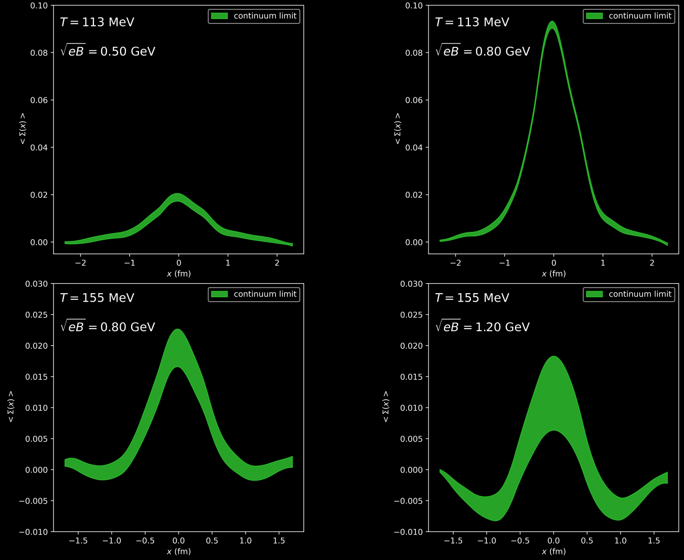

CHIRAL CONDENSATE - $\Sigma(T,B) = \frac{m_{ud}}{m_\pi^4}[\bar{\psi}\psi(T,B) - \bar{\psi}\psi(T,0)]$

What happens to the peak of the condensate as a function of T and B?

Chiral condensate - $\Sigma(T,B) = \frac{m_{ud}}{m_\pi^4}[\bar\psi\psi(T,B) - \bar\psi\psi(T,0)]$

What happens to the peak of the condensate as a function of T and B?

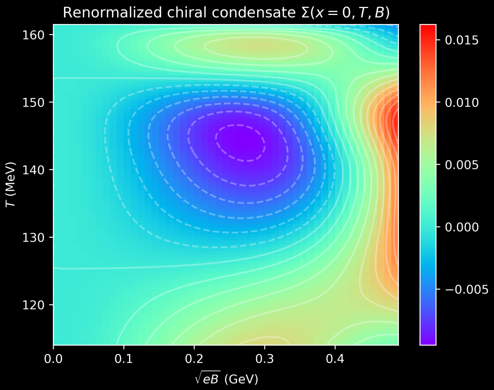

- Magnetic catalysis T away from Tc

CHIRAL CONDENSATE - $\Sigma(T,B) = \frac{m_{ud}}{m_\pi^4}[\bar{\psi}\psi(T,B) - \bar{\psi}\psi(T,0)]$

What happens to the peak of the condensate as a function of T and B?

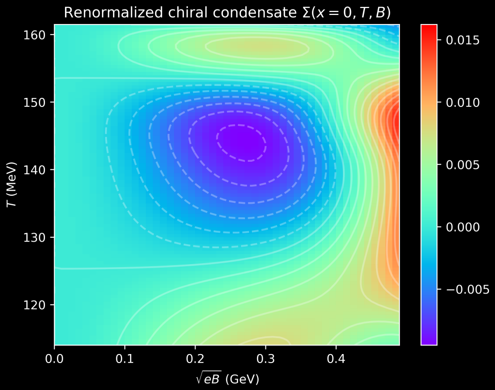

- Magnetic catalysis T away from Tc
- Inverse catalysis for T around T_c Endrődi et al. 2019

POLYAKOV LOOP - $P(x,T,B)/P(x,T,0)$

Polyakov loop - $P(x,T,B)/P(x,T,0)$

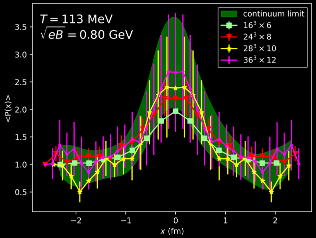

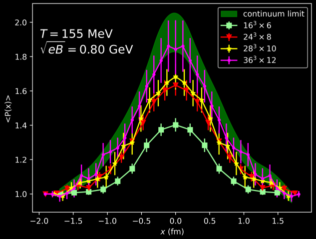

POLYAKOV LOOP - $P(x,T,B)/P(x,T,0)$

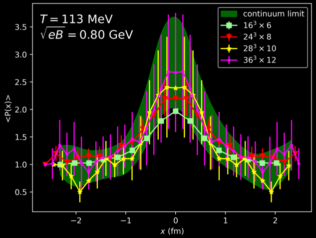

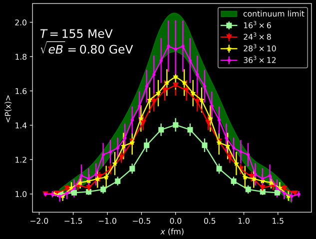

The Polyakov loop is typically broader than the chiral condensate.

POLYAKOV LOOP - $P(x,T,B)/P(x,T,0)$

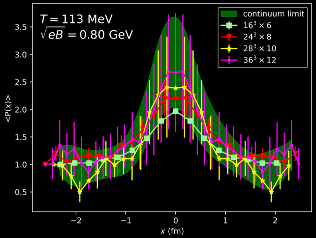

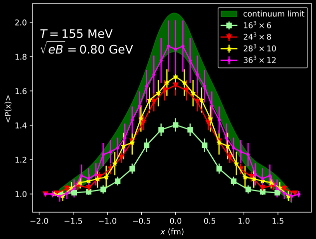

The Polyakov loop is typically broader than the chiral condensate.

$$\langle\ \bar\psi\psi(x)P(y)\ \rangle - \langle\ \bar\psi\psi(x)\ \rangle\langle\ P(x)\ \rangle$$

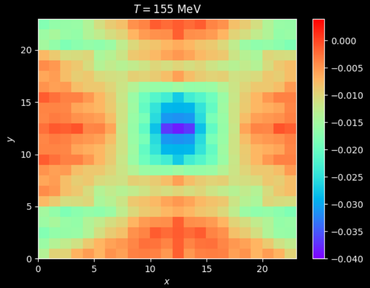

POLYAKOV LOOP - $P(x,T,B)/P(x,T,0)$

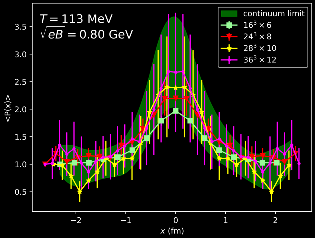

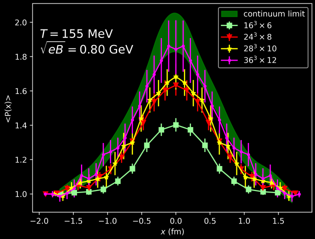

The Polyakov loop is typically broader than the chiral condensate.

$$\langle\, \bar\psi\psi(x)P(y) \,\rangle - \langle\, \bar\psi\psi(x) \,\rangle \langle\, P(x) \,\rangle$$

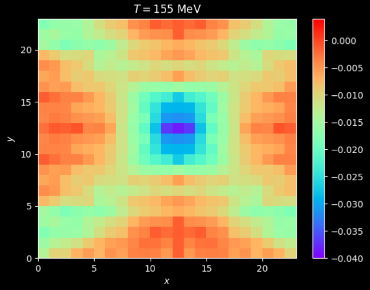

The interaction of the condensate with P causes the dips!

ELECTRIC CURRENTS - $J^i = \sum_f \frac{q_f}{e}\bar{\psi}_f \gamma^i \psi_f$

ELECTRIC CURRENTS - $J^i = \sum_f \frac{q_f}{e}\bar{\psi}_f\gamma^i\psi_f$

$\mathbf{J} \sim \boldsymbol{\nabla} \times \mathbf{B}$

ELECTRIC CURRENTS - $J^i = \sum_f \frac{q_f}{e}\bar{\psi}_f\gamma^i\psi_f$

$$\mathbf{J} \sim \boldsymbol{\nabla} \times \mathbf{B} \quad \longrightarrow \quad J_y \sim \frac{\partial B_z}{\partial x}$$

Electric currents - $J^i = \sum_f \frac{q_f}{e}\bar{\psi}_f\gamma^i\psi_f$

$$\mathbf{J} \sim \nabla \times \mathbf{B} \quad \longrightarrow \quad J_y \sim \frac{\partial B_z}{\partial x} = -\frac{2B}{\epsilon \cosh\left(\frac{x - L_x/2}{\epsilon}\right)^2} \tanh\left(\frac{x - L_x/2}{\epsilon}\right)$$

Electric currents - $J^i = \sum_f \frac{q_f}{e} \bar{\psi}_f \gamma^i \psi_f$

$$\mathbf{J} \sim \nabla \times \mathbf{B} \quad \longrightarrow \quad J_y \sim \frac{\partial B_z}{\partial x} = -\frac{2B}{\epsilon \cosh\left(\frac{x - L_x/2}{\epsilon}\right)^2} \tanh\left(\frac{x - L_x/2}{\epsilon}\right)$$

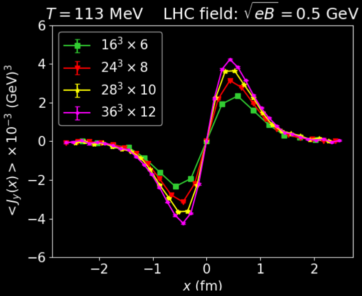

Electric currents - $J^i = \sum_f \frac{q_f}{e}\bar{\psi}_f\gamma^i\psi_f$

$$\mathbf{J} \sim \nabla \times \mathbf{B} \quad \longrightarrow \quad J_y \sim \frac{\partial B_z}{\partial x} = -\frac{2B}{\epsilon \cosh\left(\frac{x-L_x/2}{\epsilon}\right)^2}\tanh\left(\frac{x-L_x/2}{\epsilon}\right)$$

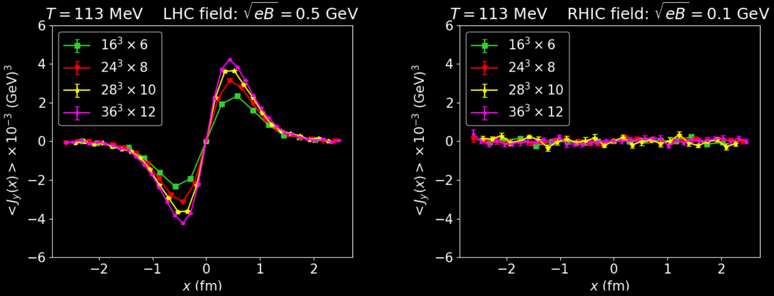

Figure 6: Lattice electric currents for LHC-like ($\sqrt{eB} = 0.5$ GeV) and RHIC-like ($\sqrt{eB} = 0.1$ GeV) magnetic fields, respectively.

(Bare) magnetic susceptibility

(Bare) magnetic susceptibility

$$\frac{1}{\mu_0}\mathbf{B} = \mathbf{H} + \mathbf{M} \quad \longrightarrow \quad \mathbf{J}_{tot} = \mathbf{J}_f + \mathbf{J}_m \quad \longrightarrow \quad \mathbf{J}_m = \nabla \times \mathbf{M}$$

(Bare) magnetic susceptibility

$$\frac{1}{\mu_0}\mathbf{B} = \mathbf{H} + \mathbf{M} \quad \longrightarrow \quad \mathbf{J}_{tot} = \mathbf{J}_f + \mathbf{J}_m \quad \longrightarrow \quad \mathbf{J}_m = \nabla \times \mathbf{M}$$

- Linear response term:
  $\mathbf{M} \approx \chi_m \mathbf{H}$

(Bare) magnetic susceptibility

$$\frac{1}{\mu_0}\mathbf{B} = \mathbf{H} + \mathbf{M} \quad \longrightarrow \quad \mathbf{J}_{tot} = \mathbf{J}_f + \mathbf{J}_m \quad \longrightarrow \quad \mathbf{J}_m = \nabla \times \mathbf{M}$$

- Linear response term:
  $\mathbf{M} \approx \chi_m \mathbf{H}$
- $\dfrac{\chi_m}{1+\chi_m} \nabla \times \mathbf{B} = \mathbf{J}_m$

(BARE) MAGNETIC SUSCEPTIBILITY

$$\frac{1}{\mu_0}\mathbf{B} = \mathbf{H} + \mathbf{M} \quad \longrightarrow \quad \mathbf{J}_{tot} = \mathbf{J}_f + \mathbf{J}_m \quad \longrightarrow \quad \mathbf{J}_m = \nabla \times \mathbf{M}$$

- Linear response term: $\mathbf{M} \approx \chi_m \mathbf{H}$
- $\frac{\chi_m}{1+\chi_m} \nabla \times \mathbf{B} = \mathbf{J}_m$

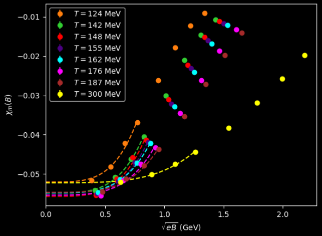

(BARE) MAGNETIC SUSCEPTIBILITY

$$\frac{1}{\mu_0}\mathbf{B} = \mathbf{H} + \mathbf{M} \quad \longrightarrow \quad \mathbf{J}_{tot} = \mathbf{J}_f + \mathbf{J}_m \quad \longrightarrow \quad \mathbf{J}_m = \nabla \times \mathbf{M}$$

- Linear response term: $\mathbf{M} \approx \chi_m \mathbf{H}$
- $\frac{\chi_m}{1+\chi_m}\nabla \times \mathbf{B} = \mathbf{J}_m$

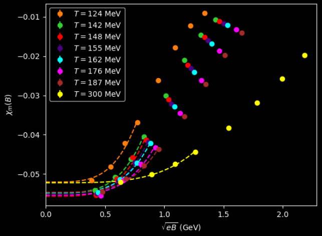

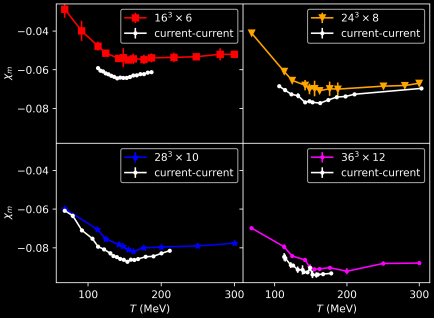

(Bare) magnetic susceptibility

$$\frac{1}{\mu_0}\mathbf{B} = \mathbf{H} + \mathbf{M} \longrightarrow \mathbf{J}_{tot} = \mathbf{J}_f + \mathbf{J}_m \longrightarrow \mathbf{J}_m = \nabla \times \mathbf{M}$$

- Linear response term: $\mathbf{M} \approx \chi_m \mathbf{H}$
- $\dfrac{\chi_m}{1+\chi_m}\nabla \times \mathbf{B} = \mathbf{J}_m$

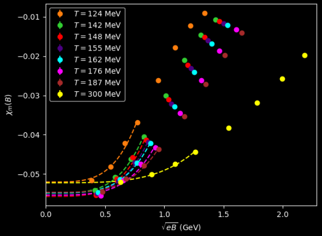

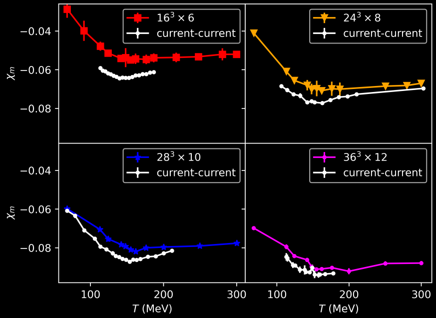

The susceptibility contains an additive divergence $\chi_m \sim \log(a)$

(Renormalized) magnetic susceptibility

The divergence is independent of T: $\chi_m^r(T) \equiv \chi_m(T) - \chi_m(0)$

(Renormalized) magnetic susceptibility

The divergence is independent of T: $\chi_m^r(T) \equiv \chi_m(T) - \chi_m(0)$

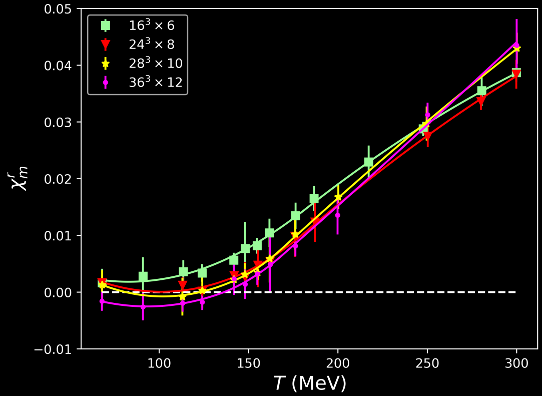

(Renormalized) magnetic susceptibility

The divergence is independent of T: $\chi_m^r(T) \equiv \chi_m(T) - \chi_m(0)$

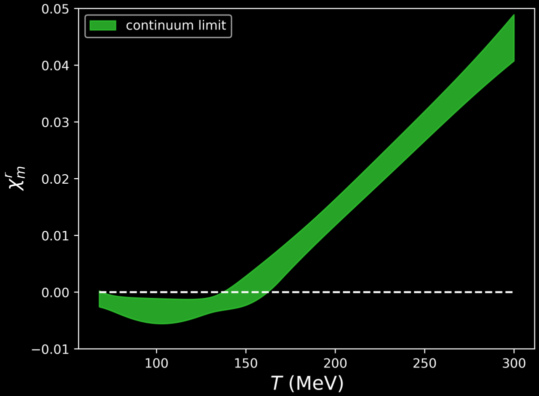

(Renormalized) magnetic susceptibility

The divergence is independent of T: $\chi_m^r(T) \equiv \chi_m(T) - \chi_m(0)$

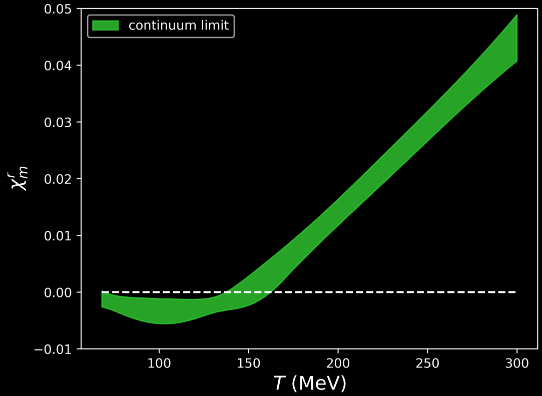

- $\chi_m^r < 0$: diamagnetism

(Renormalized) magnetic susceptibility

The divergence is independent of T: $\chi_m^r(T) \equiv \chi_m(T) - \chi_m(0)$

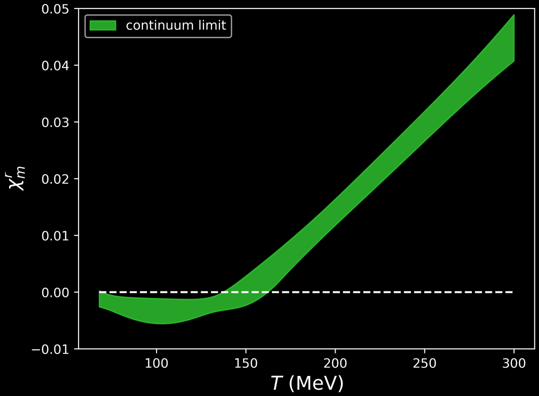

- $\chi_m^r < 0$: diamagnetism
- $\chi_m^r > 0$: paramagnetism

(Renormalized) magnetic susceptibility

The divergence is independent of T: $\chi_m^r(T) \equiv \chi_m(T) - \chi_m(0)$

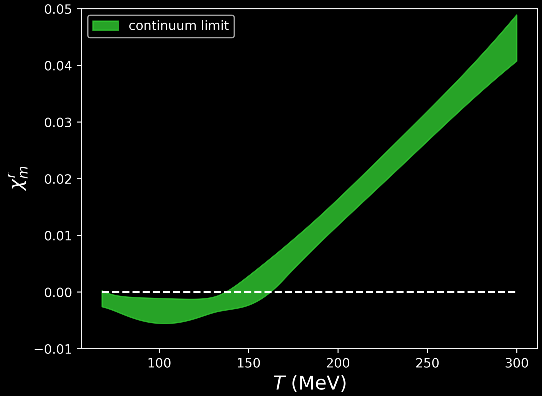

- $\chi_m^r < 0$: diamagnetism
- $\chi_m^r > 0$: paramagnetism

Material	χ_m
Al	+2.2$\times 10^{-5}$
Glass	-1.13$\times 10^{-5}$

Great agreement with the current-current method! Bali, Gergely Endrődi, and Piemonte 2020

Summary & Conclusions

SUMMARY & CONCLUSIONS

- A richer scenario emerges in the presence of an inhomogeneous B (dips, steady eletric currents, etc.);

Summary & Conclusions

- A richer scenario emerges in the presence of an inhomogeneous B (dips, steady eletric currents, etc.);
- Prominent electric currents for LHC-like magnetic fields and stronger;

Summary & Conclusions

- A richer scenario emerges in the presence of an inhomogeneous B (dips, steady eletric currents, etc.);
- Prominent electric currents for LHC-like magnetic fields and stronger;
- Using J_m and Maxwell's equations we introduced a new method to compute χ_m;

Summary & Conclusions

- A richer scenario emerges in the presence of an inhomogeneous B (dips, steady eletric currents, etc.);
- Prominent electric currents for LHC-like magnetic fields and stronger;
- Using J_m and Maxwell's equations we introduced a new method to compute χ_m;
- Our χ_m corroborates the picture of weak diamagnetism in QCD for $T < T_c$ and strong paramagnetism for $T > T_c$;

Summary & Conclusions

- A richer scenario emerges in the presence of an inhomogeneous B (dips, steady eletric currents, etc.);
- Prominent electric currents for LHC-like magnetic fields and stronger;
- Using J_m and Maxwell's equations we introduced a new method to compute χ_m;
- Our χ_m corroborates the picture of weak diamagnetism in QCD for $T < T_c$ and strong paramagnetism for $T > T_c$;
- The knowledge of these processes is important to capture the correct physics in heavy-ion collision studies (QCD models, hydrodynamics, etc.);

Summary & Conclusions

- A richer scenario emerges in the presence of an inhomogeneous B (dips, steady eletric currents, etc.);
- Prominent electric currents for LHC-like magnetic fields and stronger;
- Using J_m and Maxwell's equations we introduced a new method to compute χ_m;
- Our χ_m corroborates the picture of weak diamagnetism in QCD for $T < T_c$ and strong paramagnetism for $T > T_c$;
- The knowledge of these processes is important to capture the correct physics in heavy-ion collision studies (QCD models, hydrodynamics, etc.);
- More on electromagnetic fields in lattice QCD: talk by Javier Hernandez today at 14:50!

Bibliography I

References

- Deng, Wei-Tian and Xu-Guang Huang (2012). “Event-by-event generation of electromagnetic fields in heavy-ion collisions”. In: *Physical Review C* 85.4, p. 044907.
- Cao, Gaoqing (2018). “Chiral symmetry breaking in a semilocalized magnetic field”. In: *Physical Review D* 97.5, p. 054021.
- Endrődi, G et al. (2019). “Magnetic catalysis and inverse catalysis for heavy pions”. In: *Journal of High Energy Physics* 2019.7, pp. 1–15.

Bibliography II

Bali, Gunnar S, Gergely Endrődi, and Stefano Piemonte (2020). "Magnetic susceptibility of QCD matter and its decomposition from the lattice". In: *Journal of High Energy Physics* 2020.7, pp. 1–43.

B QUANTIZATION CONDITION

fermion fields $\longrightarrow \bar{\psi}$, ψ

gluon fields $\longrightarrow U_\mu = e^{iagA_\mu^b T_b} \in$ SU(3)

magnetic field $\longrightarrow u_\mu = e^{iaqA_\mu} \in$ U(1)

$$\mathbf{B} = B\hat{z}$$

Stoke's theorem must hold on the torus.

inner area: $\oint A_\mu dx_\mu = SB$

outer area: $\oint A_\mu dx_\mu = (L_x L_y - S)B$

$$e^{-iqBS} = e^{iqB(L_x L_y - S)}$$

$$\boxed{qB = \frac{2\pi N_b}{L_x L_y}, \quad N_b \in \mathbb{Z}}$$

(anti-)periodic BC

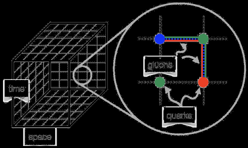

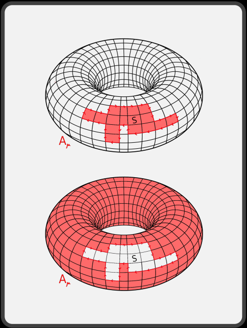

INHOMOGENEOUS $\bar{\psi}\psi(x)$ VS HOMOGENEOUS $\bar{\psi}\psi(B(x))$

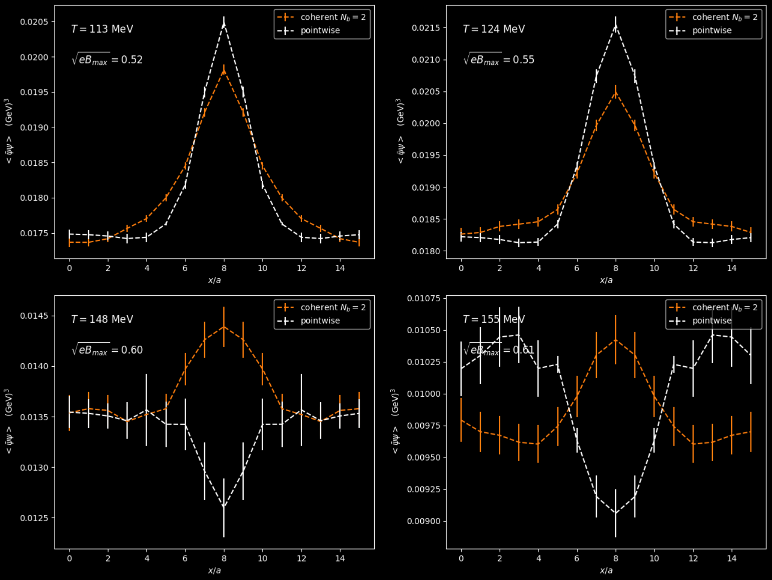

Correlations with P

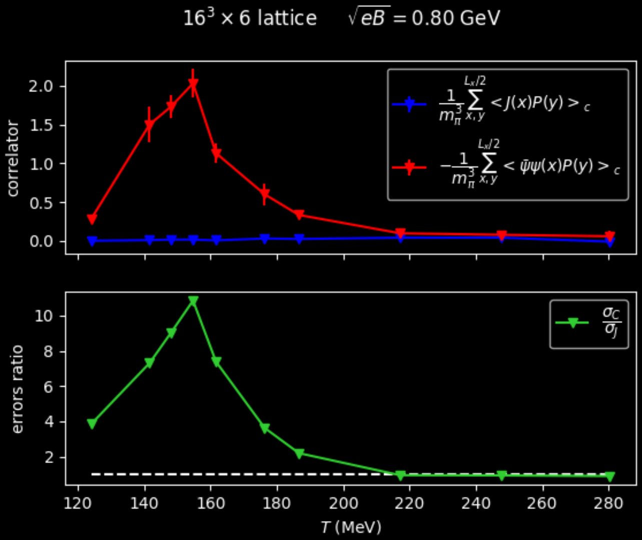

BEYOND LINEAR RESPONSE IN χ_m

$$\chi_m(B) = \chi_m(0) + \frac{c_2}{2!}B^2 + \frac{c_4}{4!}B^4 + \mathcal{O}(B^6)$$

To compute the non-linear dependence of χ_m on B

$$\mathbf{M}(\mathbf{r}) = \frac{1}{\mu_0}\int d^3x' \chi_m(\mathbf{r}, \mathbf{r}', B) B(\mathbf{r}')$$